ELSEVIER

Journal of Non-Crystalline Solids 218 (1997) 391–394

JOURNAL OF NON-CRYSTALLINE SOLIDS

Sol–gel coatings for light trapping in crystalline thin film silicon solar cells

R. Brendel [a,*], A. Gier [b], M. Mennig [b], H. Schmidt [b], J.H. Werner [c]

[a] *Max-Planck-Institut für Festkörperforschung, Heisenbergstraße 1, D-70569 Stuttgart, Germany*
[b] *Institut für Neue Materialien GmbH, Im Stadtwaldgebäude 43, D-66123 Saarbrücken, Germany*
[c] *Institut für Physikalische Elektronik, Universität Stuttgart, Pfaffenwaldring 47, D-70569 Stuttgart, Germany*

Abstract

An increase of light absorption by light trapping is a key issue for the design of thin film solar cells from crystalline silicon. According to our numerical work, the deposition of crystalline silicon layers of thickness, $W = 4$ μm, on textured glass substrates doubles the cell current for facet angles, $\alpha = 75°$, and texture periods, $p < 16$ μm, without the need for anti reflection coatings. We demonstrate the fabrication of such micron-sized light traps by embossing of sol–gel glasses. © 1997 Elsevier Science B.V.

1. Introduction

Increase of optical absorption by light trapping schemes becomes vital for thin polycrystalline silicon (c-Si) solar cells. The mechanisms of light trapping in c-Si solar cells are well understood [1,2]. Conventional thick cells are fabricated from Si wafers of thickness 200 μm $< W <$ 400 μm and are commonly textured with pyramids of period 10 μm $< p <$ 20 μm, hence $p \ll W$. Very thin cells with thickness 2 μm $< W <$ 5 μm would require sub-micron-sized textures to fall in the category $p \ll W$. Alternatively, the thin semiconductor layer can be deposited onto a substrate that is coarsely textured with a structure of period $p > W$ [3]. This approach provides excellent light trapping [4–7]; especially if the texture period p has the same order of magnitude as the thickness W [5–7]. Then, textures with periods $p \approx 10$ μm are required for c-Si films of thickness 2 μm $< W <$ 5 μm. To our knowledge the fabrication of such micron-sized textures into glass has not yet been demonstrated.

Sol–gel techniques promise an elegant way to fabricate micron-sized textures. Embossing allows one to form a wide variety of texture geometries. Therefore, this paper evaluates different texture geometries by numerical ray tracing in order to identify effective light trapping schemes. Then we describe the formation of one of those geometries by the sol–gel method.

2. Theoretical and experimental procedures

2.1. Ray tracing

Fig. 1 shows the four light trapping textures investigated in this paper: (a) the encapsulated-V texture [4] with a V-grooved glass superstrate, (b) the

* Corresponding author. Tel.: +49-711 689 1606; fax: +49-711 689 1010; e-mail: brendel@quasix.mpi-stuttgart.de.

PII S0022-3093(97)00170-1

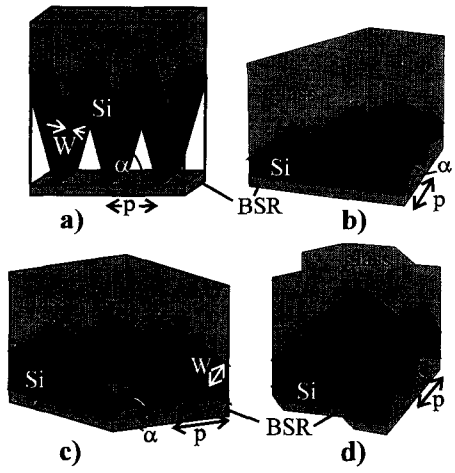

Fig. 1. The four textures investigated in this paper: (a) encapsulated-V, (b) tripyramidal-film, (c) square pyramidal-film, and (d) hexpyramidal-film. A thin Si films covers the textured glass superstrate. The period p is larger than the film thickness W. A detached back surface reflector (BSR) reduces metal reflection losses. All facets are inclined by an angle α relative to the macroscopic cell surface.

tripyramidal-film [5], (c) the square pyramidal-film [5,7], and (d) the hexpyramidal-film texture with triangular, square, and hexagonal based pyramids, respectively. The optical advantages of all these designs are: steep facets with large facet angle, α, (i) reduce the reflectance at the glass/silicon interface and (ii) increase the silicon volume available for absorption. (iii) The back surface reflector (BSR) is detached from the bottom of the silicon layer to reduce the number of reflections. All textures have no anti-reflection coatings at the air/glass and the glass/Si interface. We assume a 109 nm thick SiO_2-layer for surface passivation at the Si/air interface and assume $W = 4$ μm thick Si-layers. Our numerical results are qualitatively the same for other thicknesses, for inverted textures with the pyramidal tips pointing downwards, and for glass in between the Si layer and the BSR.

We analyze the light trapping performance of the textures shown in Fig. 1 by numerical ray tracing with our Monte Carlo ray tracing program, SUNRAYS [8]. The global AM1.5G spectrum irradiates the cell at 1000 W/m^2 and we account for the daily and yearly movement of the sun.

The texture period, p, and the facet angle, α, are the two parameters that control the feasibility of the embossing process and the light efficiency of our textures shown in Fig. 1. Therefore, we investigate the influence of p and α on the maximum short circuit current density, j_{sc}^*.

2.2. Experimental

A master stamper is formed from (100)-oriented monocrystalline silicon. We etch periodic inverted pyramids with a facet angle $\alpha = 54.7°$ and period $p = 13$ μm into the silicon surface with KOH-etch. The position of the pyramids is defined photolithographically.

Sols are synthesized from tetraethoxysilan (TEOS), trimethoxysilan (MTEOS) and silica sol (Levasil 300/30) using hydrochloric acid as catalyst for hydrolysis and condensation. After stirring the sol for 10 min in an ice bath, sols are filtered with a 0.8 μm cellulose acetate filter. We filter and coat the sol on a clean soda lime glass to obtain the gel film.

We prepare silicon caoutchouc replicas from the master stamper. This material provides adhesion of the stamper to the gel film. The stamper is pressed into the wet gel film with a well defined load. Both, stamper and gel film are dried at 100°C for 1 h, prior to stamp removal. Finally, we densify the patterned coating at 500°C for 1 h. In order to obtain crack free surface relief structures, the temperature for Si deposition should not exceed 500°C because residual CH_3-groups from the MTEOS would decompose at higher temperatures.

We deposit a microcrystalline (μc) Si layer of thickness $W = 2.8$ μm by ion assisted Si evaporation [9] at a substrate temperature of 480°C onto the textured sol–gel glass and a non-textured flat glass.

3. Results

3.1. Ray tracing

Fig. 2 shows that j_{sc}^* increases with decreasing p due to improved randomization of light propagation in structures with more ridges per cell area [5–7]. The current density j_{sc}^* saturates on a high level for $p < 4\ W$ (here: $p < 16$ μm).

Fig. 3 investigates the dependence of j_{sc}^* for small $p = 15$ μm on α. Non-textured cells ($\alpha = 0°$) of thickness, $W = 4$ μm, yield $j_{sc}^* = 20$ mA/cm^2. At

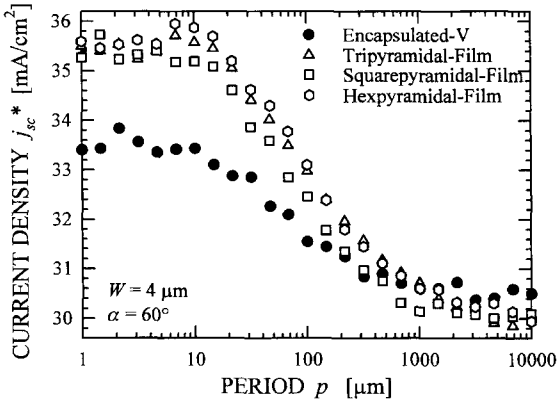

Fig. 2. All four textures show an increase in maximum short circuit current density j_{sc}^* with decreasing period p. The statistical error of the numerical j_{sc}^* data is 0.1 mA/cm^2.

$\alpha = 75°$, j_{sc}^* reaches 38 mA/cm^2. All rays of light that leave the cell structure without entering the Si at least once contribute to current loss, j_{ref}. Fig. 3 shows j_{ref} that decreases with increasing facet angle α.

3.2. Experimental

Fig. 4 shows two scanning electron microscope images of the μc-Si layer, the sol–gel glass, and the glass substrate. The patterned coating has a maximum angle $\alpha = 40°$ instead of $\alpha = 54.7°$. The measured angles vary between $\alpha = 40°$ at the ridges and $\alpha = 0°$ at the bottom of the pyramids. Optical reflectance measurements of the sample shown in Fig. 4 show an optical absorption larger than for a co-deposited flat ($a = 0°$) sample.

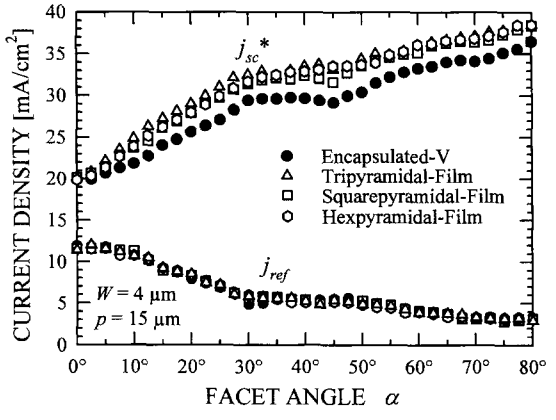

Fig. 3. Current densities j_{sc}^* of up to 38 mA/cm^2 are feasible with steep facet angles $a = 75°$ and small periods $p = 15$ μm for a layer of thickness $W = 4$ μm. The current loss j_{ref} due to surface reflectance decrease with facet angles a. The statistical error of the numerical j_{sc}^* data is 0.1 mA/cm^2, the error of j_{ref} is smaller than 0.2 mA/cm^2.

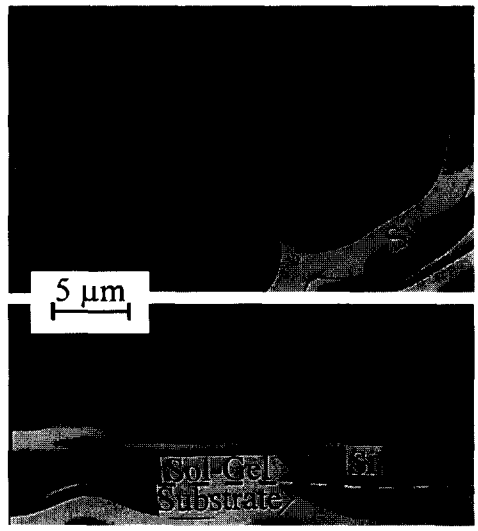

Fig. 4. Scanning electron microscope images (perspective view and cross-sectional view) of a glass micro-textured with inverted pyramids. The micro-texture is produced by embossing a sol–gel glass. The period p of the pyramids is 13 μm and the μc-Si film thickness is $W = 2.8$ μm at the bottom of the pyramids. Contrast of the Si/sol–gel interface is enhanced by a pencil line.

4. Discussion

4.1. Ray tracing

Our textures fall into two classes in Fig. 2: (i) The three-dimensional textures (3D) with a large j_{sc}^* at small p and (ii) the two-dimensional (2D) encapsulated-V texture with a smaller j_{sc}^*. The 3D-textures performs better because the average path length of light is larger. We calculate an average path length $L = (49 \pm 2.6)W_{eff}$ for the 3D textures and $L = (12 \pm 1.5)W_{eff}$ for the encapsulated-V texture. Here, $W_{eff} = W/\cos(\alpha)$ denotes the effective thickness. These values are close to the theoretical limits $L_{2D} = 4n \approx 14W_{eff}$, and $L_{3D} = 4n^2W_{eff} = 51W_{eff}$ set by the dimensionality of the texture [1] where n denotes the refractive index of Si at a wavelength of 1000 nm. The limiting value, $L_{3D} = 4n^2W_{eff}$, is reached for all

p and most α (checked with 10% accuracy). Hence, the p-dependence of j_{sc}^{*} shown in Fig. 2 is not caused by a p-dependent L, but by a p-dependent standard deviation of the path length distribution, $p(l)$, as explained in Refs. [6,10].

Fig. 2 shows that texturing almost doubles the current to be expected from the solar cell. There is no detectable difference in performance of the different 3D textures at large α. According to comprehensive transport modeling the efficiency of very thin solar cells is current controlled rather than voltage controlled [11]. Hence, large facet angles are advantageous not only in terms of current but also in terms of cell efficiency.

Fig. 3 shows j_{ref} to decrease with increasing α, since the rays of light have more attempts to enter the Si film for large α. The current loss j_{ref} is still 3 mA/cm^2 for very large α, due to the reflectance at the air/glass interface. The importance of this loss mechanism was identified by Scheydecker and his solution was to textured the front side of the glass superstrate [12]. Our calculations demonstrate that for $W = 4$ μm thick Si films current densities as high as 40 mA/cm^2 are possible for square pyramidal-film textures ($a = 75°$, $p = 15$ μm) if the front side of the glass is textured with grooves ($a = 75°$).

4.2. Experimental

The deviations of the patterned sol–gel glass from the shape of the stamper are caused by shrinkage, which results from a not yet optimized embossing process. Optimization of stamper manufacturing and embossing process are required. The sol–gel process could similarly be applied to the front side of the glass superstrate in order to reduce the reflectance at the air/glass interface.

5. Conclusions

Glass substrates textured by embossed sol–gel glasses present a novel technique to introduce light trapping schemes into thin film solar cells. According to our numerical work sol–gel processes that yield textures with large facet angles α must be developed.

Acknowledgements

We thank S. Oelting for silicon deposition, R.B. Bergmann for fruitful discussions, and H.J. Queisser for his continuous support of our photovoltaic research. This work was supported by the BMBF under contract No. 0329634.

References

[1] J.C. Miñano, in: Physical Limitations to Photovoltaic Energy Conversion, ed. A. Luque and G.L. Araùjo (Adam Hilger, Bristol, 1990) p. 50.
[2] M.A. Green, in: Advances in Solar Energy, Vol. 8, ed. M. Prince (American Solar Energy Society, Boulder, CO, 1993) p. 231.
[3] G. Schumm, H.-D. Mohring, G.H. Bauer, in: Proc. 11th European Countries Photovoltaic Solar Energy Conf., ed. L. Guimaraes, W. Palz, C. De Reyff, H. Kiess and P. Helm (Harwood Academic, Chur, 1992) p. 207.
[4] R. Brendel, in: Proc. 13th European Photovoltaic Solar Energy Conf., ed. W. Freiersleben, W. Palz, H.A. Ossenbrink and P. Helm (H.S. Stephens, Bedford, 1995) p. 436.
[5] D. Thorp, P. Campbell, S.R. Wenham, in: Proc. 25th IEEE Photovoltaic Specialists Conf. (IEEE, New York, 1996) p. 705.
[6] D. Thorp, P. Campbell, S.R. Wenham, Prog. Photovol. 4 (1996) 205.
[7] R. Bergmann, R. Brendel, M. Wolf, P. Lölgen, H.J. Werner, J. Krinke, H. Strunk, in: Proc. 25th IEEE Photovoltaic Specialists Conf. (IEEE, New York, 1996) p. 365.
[8] R. Brendel, in: Proc. 12th European Photovoltaic Solar Energy Conf., ed. R. Hill, W. Palz and P. Helm (H.S. Stephens, Bedford, 1994) p. 1339.
[9] S. Oelting, D. Martini, D. Bonnet, in: Proc. 12th European Photovoltaic Solar Energy Conf., ed. R. Hill, W. Palz and P. Helm (H.S. Stephens, Bedford, 1994) p. 1815.
[10] R. Brendel, Prog. Photovol. 3 (1995) 25.
[11] U. Rau, T. Meyer, M. Goldbach, R. Brendel, J.H. Werner, in: Proc. 25th IEEE Photovoltaic Specialists Conf. (IEEE, New York, 1996) p. 469.
[12] A. Scheydecker, A. Goetzberger, V. Wittwer, in: Proc. 10th European Photovoltaic Solar Energy Conf., ed. A. Luque, G. Sala, W. Palz, G.D. Santos and P. Helm (Kluwer, Dordrecht, 1992) p. 39.